Alex. Eng. J., Alex. Univ., Volume, 28 No.2, pp. 367 - 402 (1989)

DIRECTIONAL CONTROL OF SHIPS- SINUSOIDAL RESPONSE OF PLANE MOTIONS

M. Hanafi and Aly M. El Iraki

Department of Marine Engineering and Naval Architecture,

Faculty of Engineering, Alexandria University

Alexandria, Egypt

Abstract

A mathematical model is presented to simulate the response of the coupled yaw and sway motions of a ship to sinusoidal rudder deflection. The sinusoidal deflection is considered as an approximation of the trapezoidal wave used for the standard Z-manoeuvre. The justification of this approximation is shown to be based on the fact that the ship, as a dynamic system, acts as a low-pass frequency filter, which responds principally to the fundamental component of the Fourier expansion of the trapezoidal wave, while filtering out the higher frequency components. The effect of variations in the principal dimensions' ratios of the ship, the longitudinal position of the center of gravity (L.C.G.), the location of the center of pressure (C.P.) and the rudder area on the directional stability indices and on the response of the ship is studied. The most significantly influencing factor, not only on the stability but also on a step response, was found to be the relative locations of the L.C.G. and the C.P. A slight shift of L.C.G. forward of C.P. causes a yaw rate overshoot, whereas excessive further shift of L.C.G. results in oscillating yaw rate. On the contrary, excessive shifting of L.C.G. aft of C.P. renders the ship directionaly unstable.

Nomenclature

a	translational acceleration of C.G. of ship perpendicular to velocity vector
A_r	rudder area
A.C.	Admirality Coefficient
B	ship's breadth
c_b	ship's block coefficient
D	ship's draft
d	longitudinal distance between C.G. of ship and the center of pressure; positive if forward of C.G.
F	propeller thrust
f	frictional resistance coefficient in Froude's formula
J	polar mass moment of inertia of ship about a vertical axis through C.G. including added moment of inertia due to yaw
j	$\sqrt{-1}$
k	2D/L
K_{cL}	hydrodynamic lateral force on rudder per unit radian of rudder deflection
K_D	total drag force on ship acting in the center of pressure
K_f	hydrodynamic damping torque coefficient on ship for yawing
K_L	hydrodynamic lateral force on ship per unit radian of drift angle; acting in the center of pressure
L	ship's length
l	longitudinal distance between C.G. of ship and point of action of hydrodynamic force on rudder
L.C.G.	longitudinal position of center of gravity of ship; positive if aft of midship
m	mass of ship including added mass in sway
Q.P.C.	Quasi propulsive coefficient

r	radius of gyration for the polar moment of inertia of ship
R_f	frictional resistance of ship
R.A.R.	rudder area ratio = A_r/LD
S	wetted surface area of ship at draft D
s	laplacian operator
SHP	shaft horsepower
t	time
V	ships speed
α	drift angle
α_1 ,α_2	poles of the ship's transfer functions
Δ	displacement of ship (in tons)
δ_r	rudder angle
η_h	hull efficiency
θ_m	yaw (heading) angle
θ_p	course angle
ρ	density of water
ω	frequency of sinusoidal rudder deflection and ship's response
∇	displacement volume (in ft^3)
$\dot{(\ )}$	differentiation with respect to t

1. Introduction

The treatment of the directional stability of ships was dealt with in a simple preliminary manner as early as 1922 [1], where only the conditions for stability were discussed. Since then the problem of directional stability was further developed by many authors. This has lead to both studying the hydrodynamic behavior of the ship as well as defining standard tests for manoeuvrability.

The Z-manoeuvre is one of these standard tests. Basically, the

manoeuvre is executed through deflecting the rudder in a trapezoidal wave. This trapezoidal periodic function can be expanded by Fourier theorem in a series of sine waves. The first term in the summation is the fundamental component of the expansion. Higher components will be filtered out as will be shown. Therefore, an analytic study is carried out for investigating the response of the ship to a sinusoidal rudder deflection at different frequencies covering all possible rudder deflection rates.

Sinusoidal tests, moreover, are normally performed to experimentally identify the transfer function and time constants of ships or models [2,3] in the frequency domain.

In this work an analytic solution for the frequency response of a ship to sinusoidal rudder deflection is given. Absolute stability of the problem of ship steering is discussed. The coupled sinusoidal sway and yaw responses to a sinusoidal rudder deflection input at different frequencies are derived and displayed to examine the response characteristics for different ship parameters. Variations in length-draft ratio, length-breadth ratio, rudder area ratio and position of the center of pressure were considered. Moreover, the effect of the added mass in sway on shifting the center of gravity of ship is also discussed.

The results are displayed graphically in polar, log-magnitude versus log ω, Bode, db-magnitude versus phase angle plots and on Nichol's chart.

2. Mathematical Model

Considering a ship travelling at a constant speed V with the rudder

set to an angle δ_r, the forces and moments acting on the ship, together with the angles describing its orientation in an inertial coordinate system is shown in Fig. (1). The ship executes in this case both translational and rotational motion. The velocity and accelerations of the C.G. of the ship with respect to the inertial coordinate system are shown in Fig. (2a) and (2b) respectively. Combined sway and yaw motions will be considered, since for linearized models the remaining motions, namely surge, pitch, heave and roll are uncoupled from yaw and sway motions [3]. In [4] this problem was dealt with, however no results were given.

Applying d'Alembert's principle in the direction perpendicular to the velocity vector, the differential equation for sway is obtained as

$$ma - K_L \alpha - F \cos(90 - \alpha) + K_{cL} \delta_r = 0 \qquad (1)$$

From Fig. (2a) the velocity vector of the ship is expressed as

$$\vec{V} = V \cdot e^{j(\frac{\pi}{2} - \theta_p)}$$

and from Fig. (2b) the total acceleration of the C.G. is

$$\frac{d}{dt}\left[V e^{j(\frac{\pi}{2} - \theta_p)} \right] = \frac{dV}{dt} e^{j(\frac{\pi}{2} - \theta_p)} + V\left[-j \frac{d\theta_p}{dt} e^{j(\frac{\pi}{2} - \theta_p)}\right],$$

from which the acceleration "a" perpendicular to the direction of V is

$$a = V \left[- j \frac{d\theta_p}{dt} \cdot e^{j(\frac{\pi}{2} - \theta_p)} \right].$$

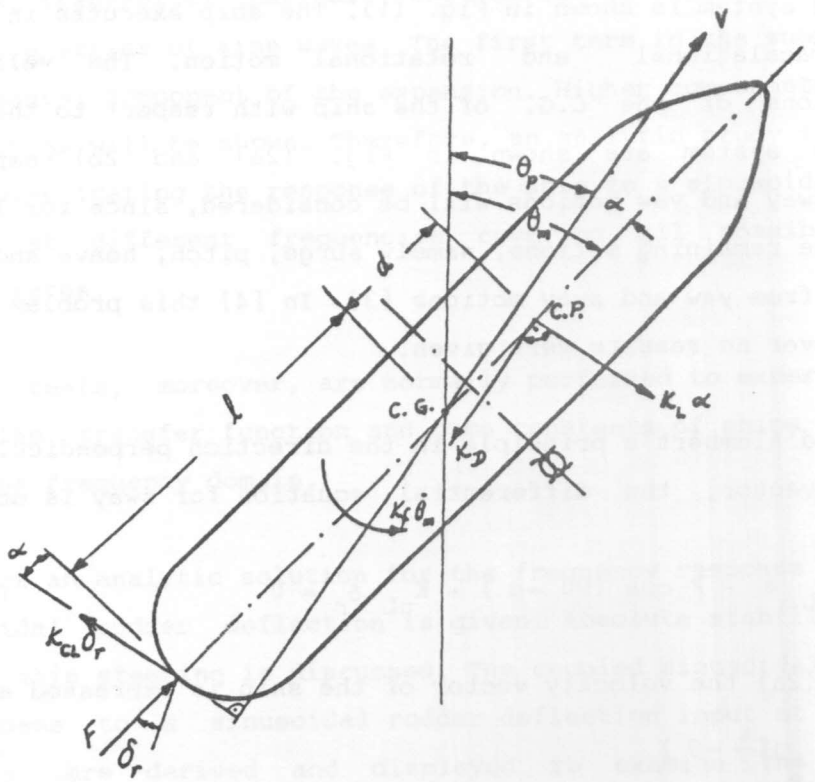

Fig. (1) Coordinates, hydrodynamic forces and torques acting on the ship

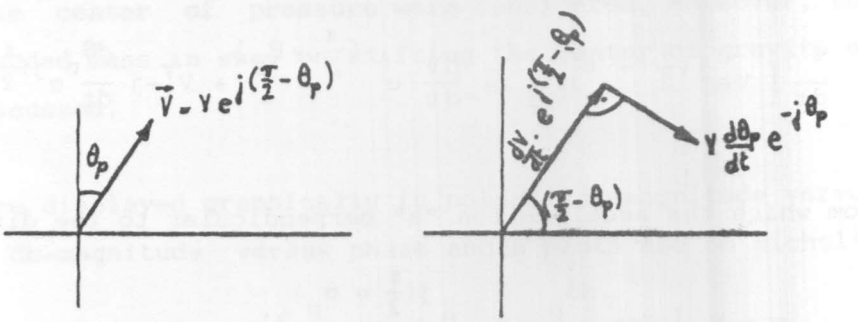

a) Velocity vector b) Acceleration vectors

Fig. (2) Velocity and acceleration diagrams

Substituting this expression for "a" Eqn. (1), noting that

$$-j = e^{j\frac{3\pi}{2}}$$

and after linearization on the assumption that α and δ_r are considered to be small angles, we obtain

$$mV\frac{d\theta_p}{dt} = (K_L + F)\alpha - K_{cL}\delta_r \qquad (2)$$

Similarly the yaw equation of motion is obtained by applying d'Alembert's principle for equilibrium of moments about C.G. as

$$J\frac{d^2\theta_m}{dt^2} - K_L\alpha\, d\cos\alpha - K_D\, d\sin\alpha - K_D\, d\sin\alpha - K_{cL}\delta_r\, \ell\cos\alpha - K_f\frac{d\theta_m}{dt} = 0$$

or after linearization for small δ_r and α angles

$$J\frac{d^2\theta_m}{dt^2} = (K_L+K_D)d\,\alpha + K_{CL}\,\ell\,\delta_r - K_f\frac{d\theta_m}{dt} \qquad (3)$$

Solving the sway and yaw equations, Eqs. (2) and (3), taking into account that the drift angle

$$\alpha = \theta_m - \theta_p$$

and after taking Laplace transform, with zero initial conditions, the following two transfer functions are obtained

$$\frac{\theta_m(s)}{\delta_r(s)} = \frac{K_{cL}[m\,\ell\,Vs + (K_L+K_D)d + (K_L+F)\ell\,]}{s\{\,JmVs^2+[J(K_L+F)+K_f mV]s+K_f(K_L+F)-mV(K_L+K_D)d\,\}} \qquad (4)$$

and

$$\frac{\theta_p(s)}{\theta_m(s)} = \frac{-Js^2 - K_f s + [(K_L+K_D)d + (K_L+F)\ell\ ]}{m\ \ell V s + [(K_L + K_D)d + (K_L+F)\ell\ \ ]} \quad . \tag{5}$$

The transfer function between the yaw rate $\dot{\theta}_m$ and δ_r can be obtained from Eqn. (4) as

$$\frac{\dot{\theta}_m(s)}{\delta_r(s)} = \frac{K_{CL}[mV\ \ell s + (K_L+K_D)d + (K_L+F)\ell\ ]}{\{JmVs^2 + [J(K_L+F)+K_f mV]s + K_f(K_L+F) - mV(K_L+K_D)d\}} \tag{6}$$

Multiplying Eqns. (4) and (5) yields the transfer function relating $\theta_p(s)$ and $\delta_r(s)$

$$\frac{\theta_p(s)}{\delta_r(s)} = \frac{K_{CL}\{-Js^2 - K_f s + [(K_L+K_D)d+(K_L+F)\ell\ ]}{s\{JmVs^2+[J(K_L+F)+K_f mV]s+K_f(K_L+F)-mV(K_L+K_D)d\}} \tag{7}$$

An obligatory condition for the directional stability of the ship is that all the roots of the characteristic equation, i.e. the denominator of Eqn. (4) or (6) set equal to zero, must have negative real parts, which necessiates that

$$K_f\ (K_L + F) > mV\ (K_L + K_D)$$

Eqn. (4) represents a $(PI)_2$-control property, Eqn. (6) a $(PD)_2$-control property and Eqn. (7) a $(PI(-D))_2$-control property.

The rudder input for a Z-manoeuvre has the form of a trapezoidal wave. Approximation of the trapezoidal wave was considered in [5] where an

idealization into pulses was treated. Another approach will be adopted here.

In order to approximate the Z-manoeuvre, the trapzoidal wave is expanded by Fourier series in the form

$$\delta_r(t) = \frac{4\,\bar{\delta}_r}{\pi\, t_r\, \omega} \sum_{n=1,3,5,\ldots}^{\infty} \frac{\sin n\omega t_r}{n^2} \sin n\omega t$$

where t_r is the time required to deflect the rudder an angle equal to $\bar{\delta}_r$ and ω is the frequency of the trapezoidal wave. The predominant harmonic in this expansion is the fundamental component with the lowest frequency , which possesses the largest amplitude.

The transfer function G(s) of a real controlled plant can be expressed as a fractional rational function in which the degree of the denominator is higher than the degree of the numerator, i.e the number of poles is greater than the number of zeros. This is attributed to the fact that the requirement of physical realizability imposes the limitation that

$$\lim_{s \to \infty} G(s) = 0$$

because a real plant can not follow extremely high frequencies.

The terms containing the laplacian operator s in the denominator of the transfer function of a real system cause the phase shift in a harmonic signal. The influence of such terms is more propounced, the higher its order and the larger its coefficients. The numerator of the

transfer function of a real controlled plant may have derivative elements, namely the terms containing the operator s. These elements produce a negative phase shift.

In contrast to physical systems, ideal controllers (without lags) contain derivative elements which would behave as a high-pass frequency filter and would amplify primarily the high frequency components of the input harmonic signal [6]. Besides, systems having either D_o or D_1 property behave as high-pass frequency filters as may be deduced from corresponding frequency response plots [7].

Since the transfer functions of the plane motions of the ship simulated in Eqns. (4), (6) and (7) represent $(PI)_2$, $(PD)_2$ and $(PI(-D))_2$ properties, respectively, the low-pass frequency behavior is insured. This means that the modulus of the frequency function considerably decreases with increasing frequency.

Therefore, the rudder deflection $\delta_r(t)$ is considered to be a sinusoidal function and the problem of steering is investigated by frequency response methods.

Converting the transfer functions represented by Eqns. (4), (6) and (7) to frequency functions through replacing the laplacian operator s by $j\omega$, and introducing the following frequencies related to the system time constants, in order to simplify the mathematical model [8],

$$\omega_c = \sqrt{\frac{K_{cL}\ell}{J}} \qquad \text{(rad/sec)} \qquad (8)$$

$$\omega_L = \frac{K_L + F}{mV} \quad \text{(rad/sec)} \tag{9}$$

$$\omega_{cL} = \frac{K_{cL}}{mV} \quad \text{(rad/sec)} \tag{10}$$

$$\omega_s = \sqrt{\frac{(K_L + K_D)\, d}{J}} \quad \text{(rad/sec)} \tag{11}$$

$$\omega_d = \frac{K_f}{J} \quad \text{(rad/sec)} \tag{12}$$

$$\omega_n = \sqrt{\frac{K_f(K_L+F) - mVd(K_L+K_D)}{JmV}} = \sqrt{\omega_d \cdot \omega_L - \omega_s^2} \quad \text{(rad/sec)} \tag{13}$$

we obtain

$$\frac{\theta_m(j\omega)}{\delta_r(j\omega)} = \frac{\omega_c^2 \left[j\omega + \left(\omega_L + \left(\frac{\omega_s}{\omega_c}\right)^2 \omega_{CL}\right)\right]}{j\omega\left[(j\omega)^2 + j\omega(\omega_d + \omega_L) + (\omega_d \cdot \omega_L - \omega_s^2)\right]} \tag{14}$$

$$\frac{\dot{\theta}_m(j\omega)}{\delta_r(j\omega)} = \frac{\omega_c^2 \left[j\omega + \left(\omega_L + \left(\frac{\omega_s}{\omega_c}\right)^2 \omega_{CL}\right)\right]}{\left[(j\omega)^2 + j\omega(\omega_d + \omega_L) + (\omega_d \cdot \omega_L - \omega_s^2)\right]} \tag{15}$$

$$\frac{\theta_p(j\omega)}{\delta_r(j\omega)} = \frac{-\omega_{cL}(j\omega)^2 - \omega_d \cdot \omega_{cL}(j\omega) + (\omega_s^2 \cdot \omega_{cL} + \omega_L \cdot \omega_c^2)}{j\omega\left[(j\omega)^2 + j\omega(\omega_d + \omega_L) + (\omega_d \cdot \omega_L - \omega_s^2)\right]} \tag{16}$$

and

$$\frac{\alpha(j\omega)}{\delta_r(j\omega)} = \frac{\theta_m(j\omega)}{\delta_r(j\omega)} - \frac{\theta_p(j\omega)}{\delta_r(j\omega)}$$

$$= \frac{(j\omega)\,\omega_{cL} + (\omega_c^2 + \omega_d \cdot \omega_{cL})}{\left[(j\omega)^2 + (j\omega)(\omega_d + \omega_L) + (\omega_d \cdot \omega_L - \omega_s^2)\right]} \tag{17}$$

Finally the inverse frequency function of α is

$$\frac{1}{\alpha\,(j\omega)\,/\,\delta_r\,(j\omega)} \quad .$$

3. Computational Treatment

In Eqns. (2) and (3) the coefficients depend on the hydrodynamic characteristics of the ship and the rudder.

The mass to be considered is the virtual mass of the ship including the added mass. Also the polar mass moment of inertia includes the added moment of inertia. The added mass in sway and the added mass polar moment of inertia are both approximately equal to the actual ship's mass and polar moment of inertia respectively [9].

Hence,

$$m = 2\,\rho\ L\ B\ D\ c_b$$

where c_b is calculated from Alexandar formula, namely

$$c_b = 1.08 - \frac{V}{2\sqrt{L}} \qquad \text{(V in knots, L in ft)}$$

and $J = mr^2$

where r, the radius of gyration, is given by [10]

$$r = L/4 \ .$$

The drag force K_D on the ship is assumed to be equal to the frictional resistance [9], and is independent of the drift anle [4]. The frictional resistance can be calculated using Froude's formula

$$R_f = f\ S\ V^{1.825}$$

where S is the wetted surface area in ft^2, V is ship's speed in knots and f is an emperical constant. The wetted surface area S (in ft^2) can be calculated using Denny formula, namely

$$S = (1.7\ LD + \frac{\nabla}{D}) \frac{1}{(3.28)^2} \quad (m^2)$$

where L and D in ft, ∇ in ft^3

The thrust is calculated using the Admirality coefficient relations, namely

$$A.C. = 10\ (\sqrt{L} + \frac{150}{V}) \qquad (L \text{ in ft, } V \text{ in knots})$$

and

$$SHP = \frac{\Delta^{2/3}\ V^3}{A.C.} \qquad (V \text{ in knots})$$

Hence the thrust F is given by

$$F = \frac{SHP \times Q.P.C. \times 75 \times 9.81}{\eta_h \cdot V} \qquad (N) \quad (V \text{ in m/sec})$$

The hydrodynamic damping torque coefficient in yaw is given by [11]

$$K_f = (0.54 - k)\, k\, \frac{\rho}{2} L^3 DV, \qquad \left(\frac{N.m.sec}{rad}\right)$$

where

$$k = \frac{2D}{L}$$

The hydrodynamic lateral force per unit radian of drift angle acting in the ship's center of pressure is

$$K_L = \frac{\rho}{2} L\, D\, V^2 \frac{\partial K_L}{\partial \alpha}, \qquad (N/rad)$$

where $\frac{\partial K_L}{\partial \alpha}$ is given by Jones' formula [10] as

$$\frac{\partial K_L}{\partial \alpha} = \frac{\pi}{2} k .$$

The hydrodynamic rudder force per unit radian of rudder angle is given similarly by

$$K_{cL} = \frac{\rho}{2} A_r V^2 \frac{\partial K_{cL}}{\partial \delta_r} \qquad (N/rad)\ (A_r \text{ in } m^2,\ V \text{ in m/sec})$$

For the numerical computations a ship with the following data was considered:

L	= 200 m (= 656 ft)
L/B	= 6.0 , 6.5 , 7.0
L/D	= 16, 19 , 22
Rudder area	= 0.015 LD , 0.025 LD
V	= 16 knots = 8.24 (m/sec)

d = 0.026 L, 0.033 L forward of L.C.G. [10]

f = 0.008703 (Corresponding to ship's length, salt water)

Q.P.C. = 0.6

η_h = 1.03 (single screw)

$\frac{\partial K_{cL}}{\partial \delta_r}$ = 0.022 (for rudder aspect ratio = 5)

The longitudinal distance from L.C.G. of ship to the C.G. of added lateral mass in sway varies from 0.039 L to 0.049 L [10], here an average value of 0.044 L was considered. On such basis the position of the resultant center of gravity of the ship and added mass together is located at 0.007 L forward of midship.

4. Results and Discussion

The numerical computation were carried put using a FORTRAN IV program run on the PDP-11 of the Faculty of Engineering,Alexandria University.

Figures (3) and (4) illustrate the effect of variations in L/B, L/D, location of L.C.G. and the center of pressure on the course stability of the ship expressed in terms of the poles α_1 and α_2 of the transfer function. It is evident that one of the roots is relatively small with respect to the other one. Absolute stability is ensured since the poles are all negative. This is to be expected for a ship whose parameters lie in the normal ranges. The predominant pole is α_1, since it is nearer to the instability region, thus considerably affecting the magnitude ratio and phase shift. From these figures it can be seen that increasing L/B improves the course stability, while on the other hand, increasing L/D has an opposite effect. The effect of the location of the center of pressure relative

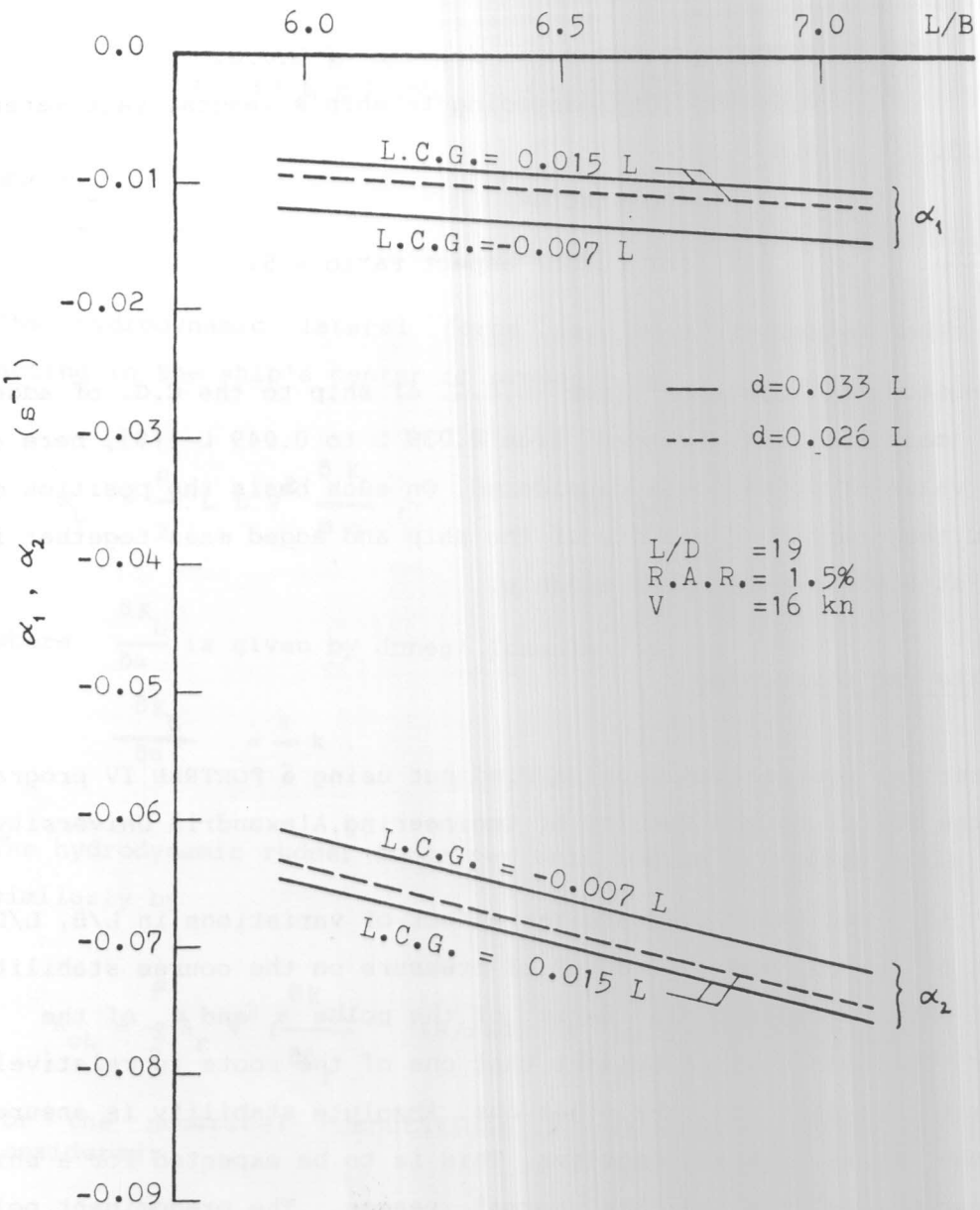

Fig. (3) Effect of variations of L/B and position of center of pressure on the poles of the transfer function, Eqn. (6).

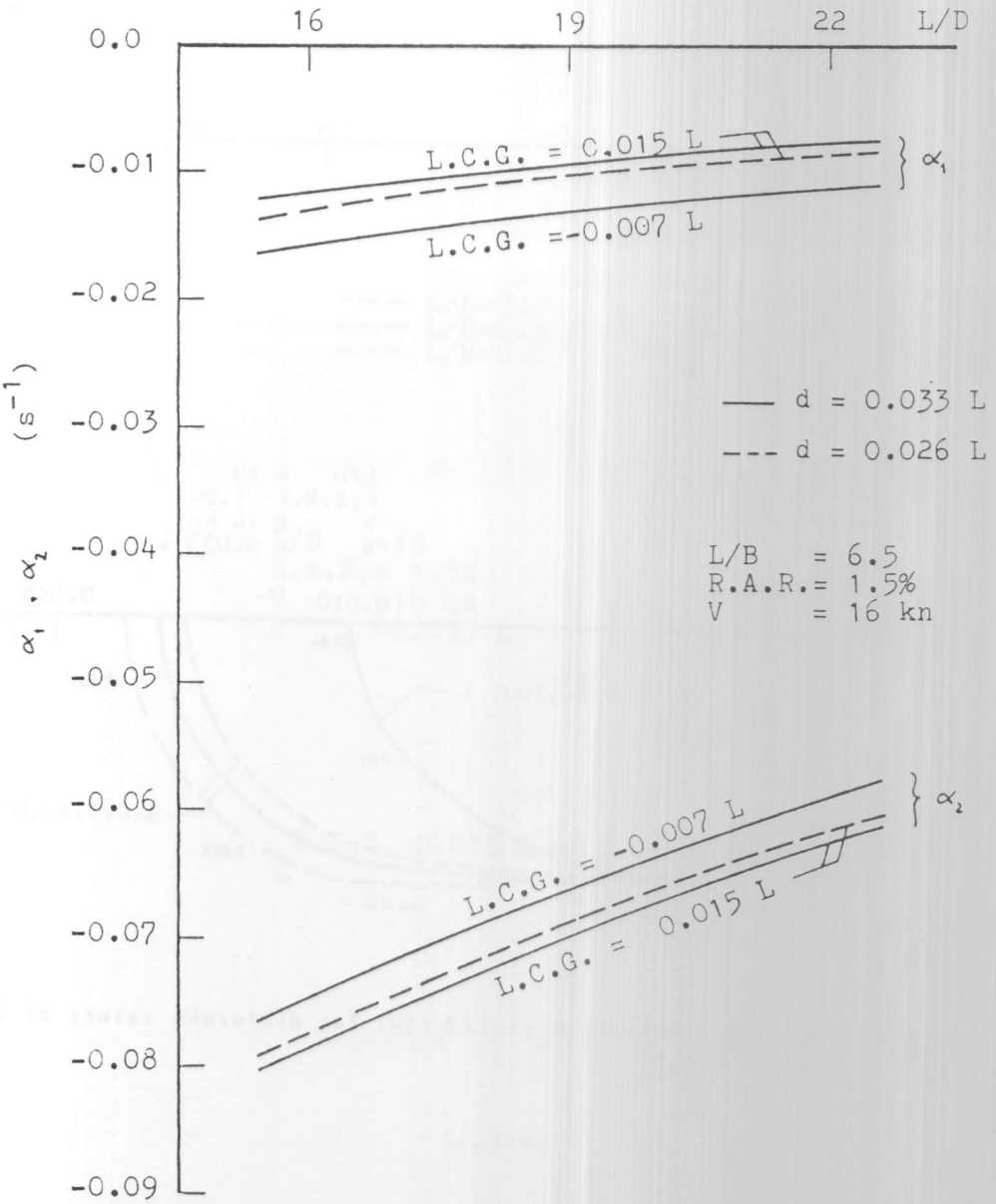

Fig. (4) Effect of variations of L/D and position of center of pressure on the poles of the transfer function. Eqn. (6).

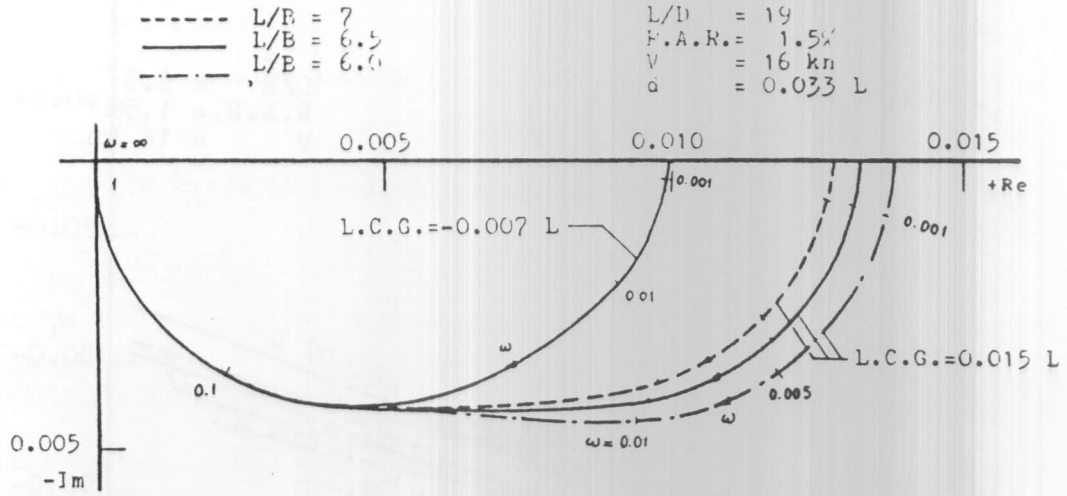

Fig. (5) Polar plots of $\dot{\theta}_m(jw)/\delta_r(jw)$ for different values of L/B and L.C.G.

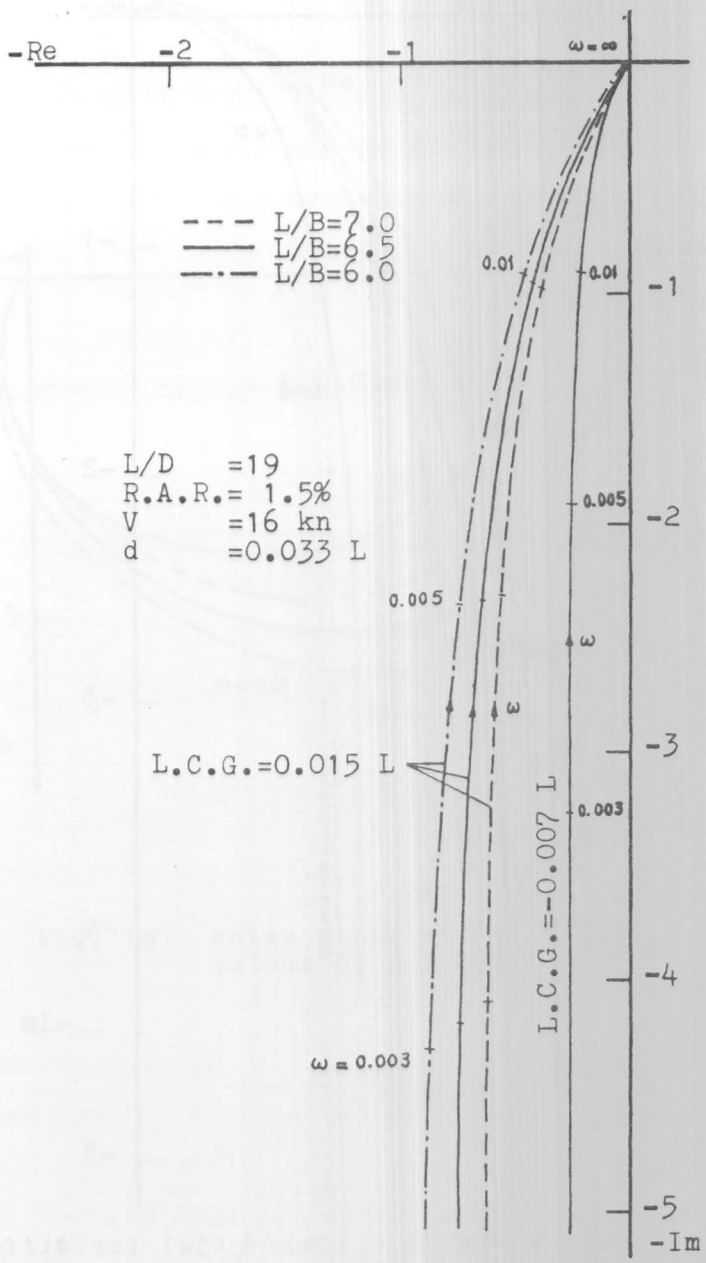

Fig. (6) Polar plots of $\theta_m(jw)/\delta_r(jw)$ for different values of L/B and L.C.G.

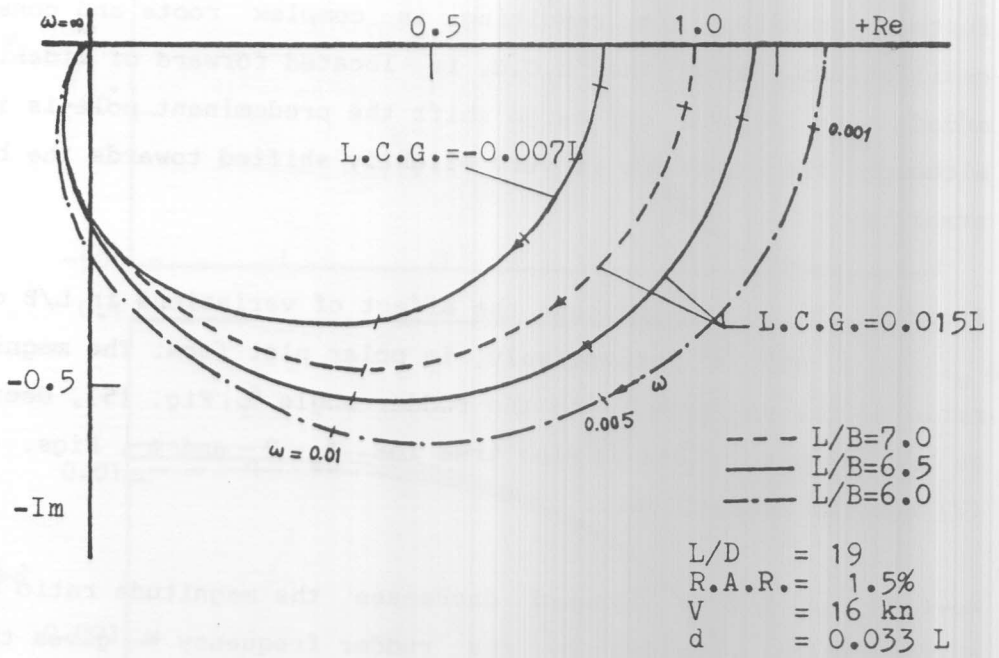

Fig. (8) Polar plots of $\alpha(jw)/\delta_r(jw)$ for different values of L/B and L.C.G.

to the L.C.G. was relatively slight in the considered range. However, decreasing the distance between the center of pressure and the L.C.G improves the course stability. Moreover, it is deduced from the results that excessive movement of the center of pressure forward of the center of pressure would render the system unstable, while moving it aft of the C.G. starts with producing some overshoot, and with further transfer aft resulting in complex roots and consequently oscillations. When the L.C.G. is located forward of midship due to added mass effect or cargo shift the predominant pole is improved, although the other one is very slightly shifted towards the border of stability.

Figures (5) to (8) indicate the effect of variations in L/B on $\dot{\theta}_m$, θ_m, θ_p, and α respectively, in polar plot form. The magnitude ratio of the yaw rate $\dot{\theta}_m$ to the rudder angle δ_r, Fig. (5), decreases as L/B increases. This is also true for θ_m, θ_p and α, Figs. (6), (7) and (8) respectively.

Moving the L.C.G. forward decreases the magnitude ratio and phase shift, which, divided by the rudder frequency ω gives the time delay between the sinusiodal ship's response and the sinusoidal rudder input.

The effect of variations in L/D on $\dot{\theta}_m$, θ_m and α is illustrated in Figs. (9) to (11) respectively, in the form of log-magnitude versus log ω, Fig. (9), and Bode diagrams, Figs (10) and (11). Increasing L/D increases the magnitude ratio of all responses and increases the negative phase shift. The shape of the magnitude ratio curves demonstrate the property of the ship as being a low-pass frequency filter.

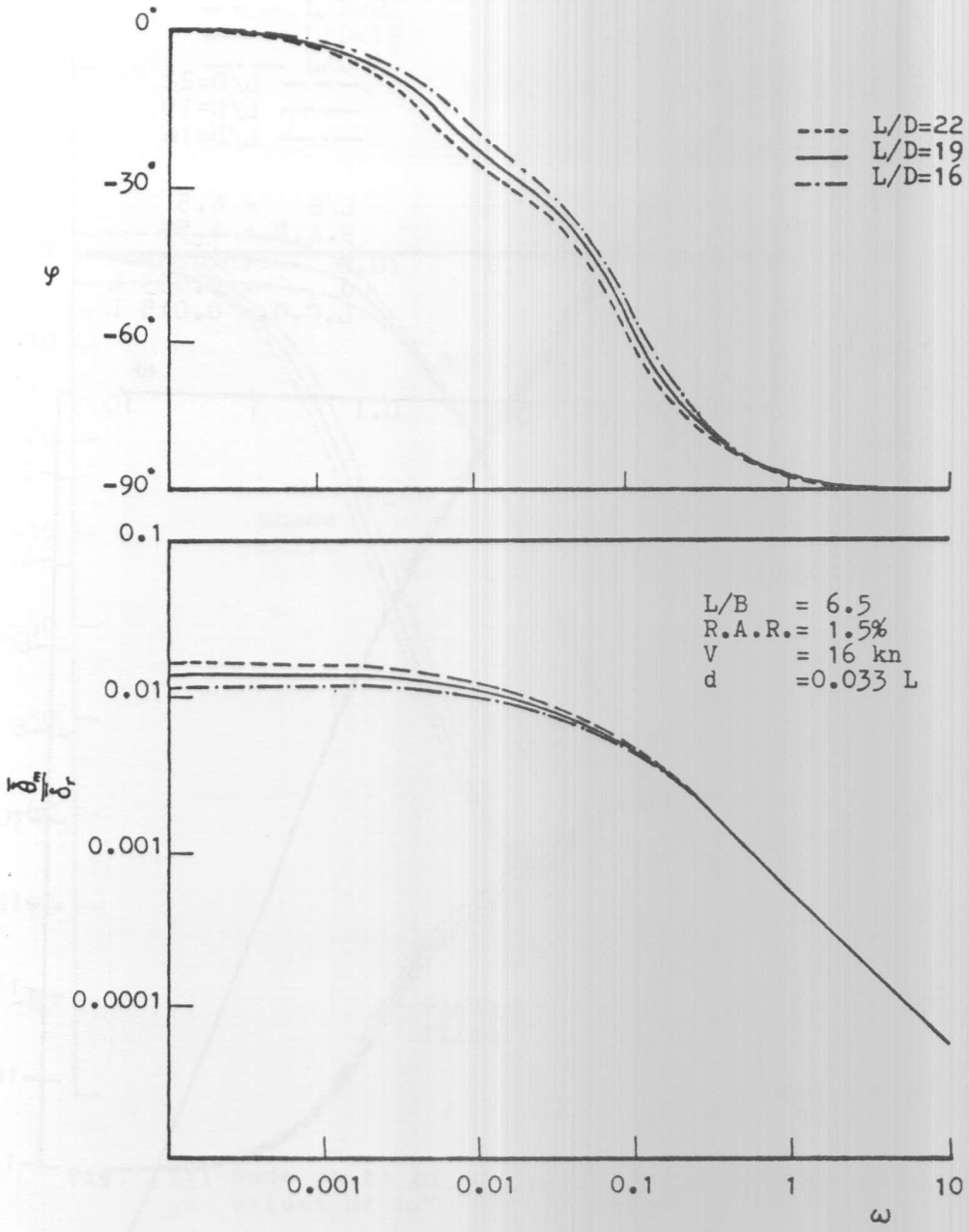

Fig. (9) Magnitude ratio and phase shift plots for $\dot{\theta}_m(jw)/\delta_r(jw)$ for different values of L/D

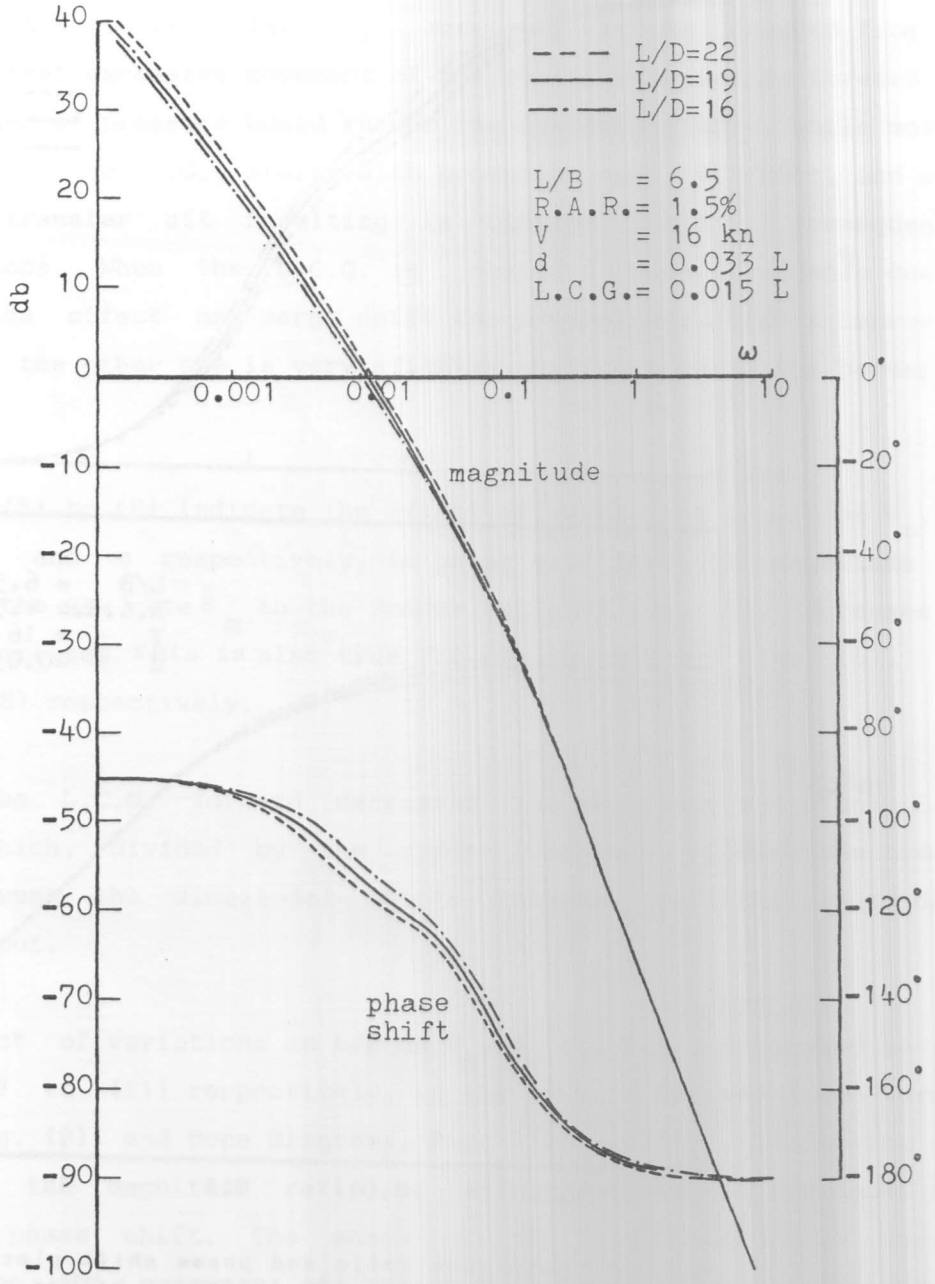

Fig. (10) Bode plots of $\Theta_m(jw)/\delta_r(jw)$ for different values of L/D

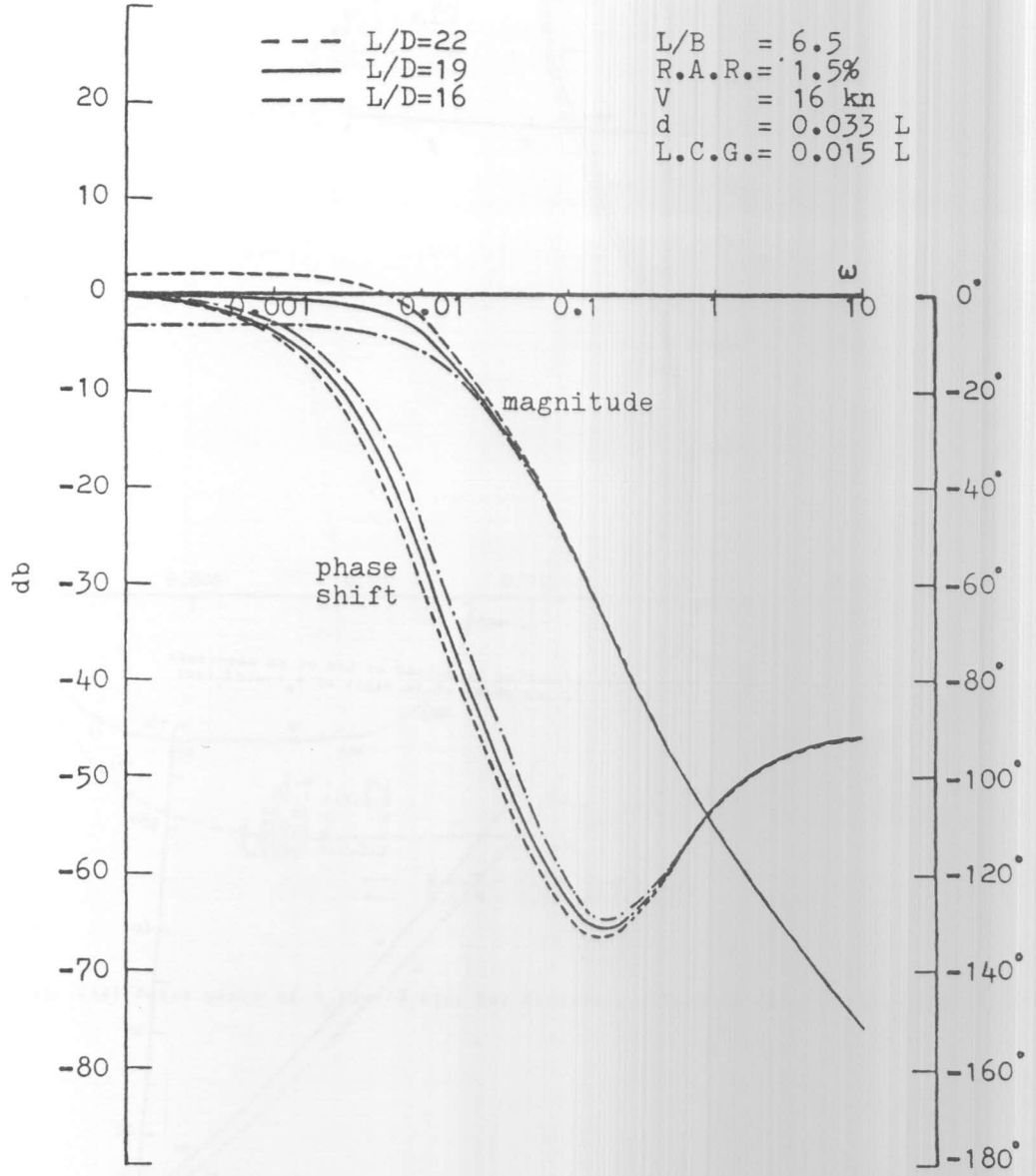

Fig. (11) Bode plots of $\alpha(jw)/\delta_r(jw)$ for different values of L/D

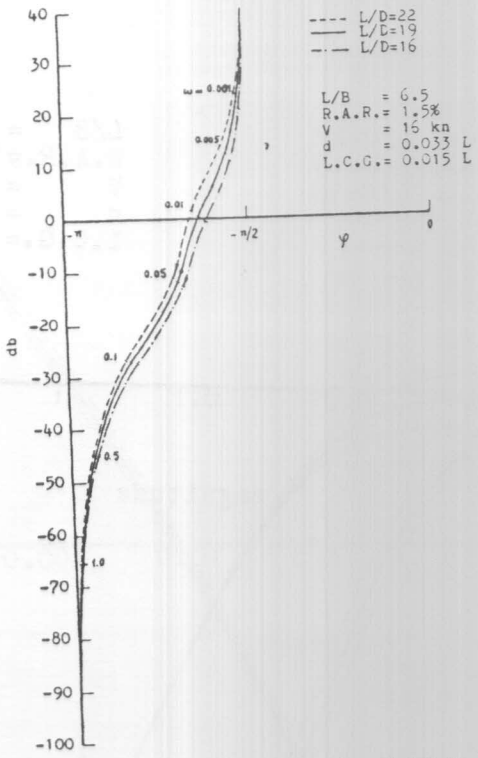

Fig. (12) Effect of variation of L/D on db magnitude versus phase shift plots of $\theta_m(jw)/\delta_r(jw)$

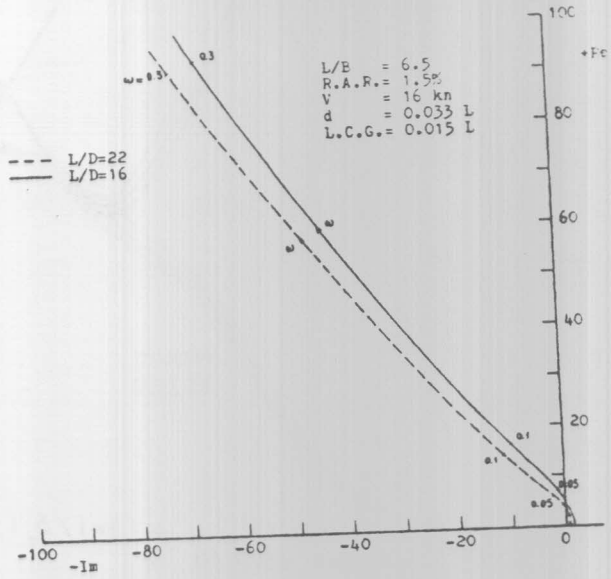

Fig. (13) Effect of variation of L/D in inverse polar plot for $\alpha(jw)/\delta_r(jw)$

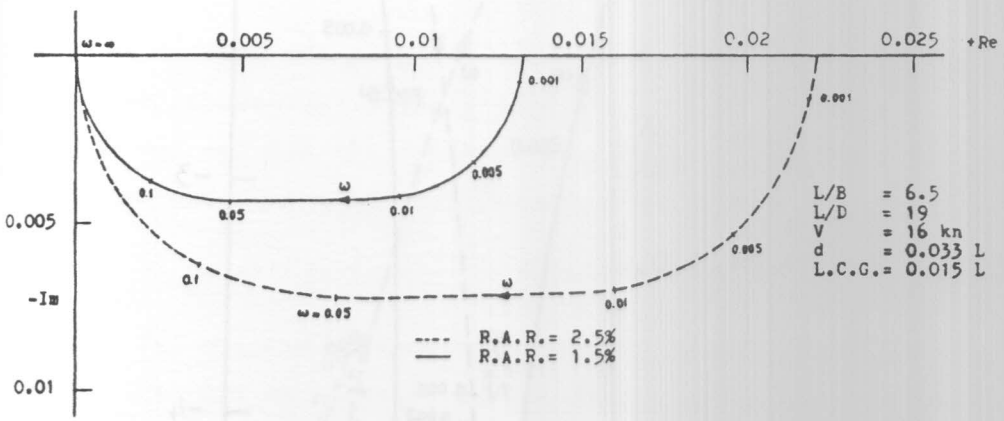

Fig. (14) Polar plots of $\dot{\theta}_m(jw)/\delta_r(jw)$ for different values of rudder area ratio

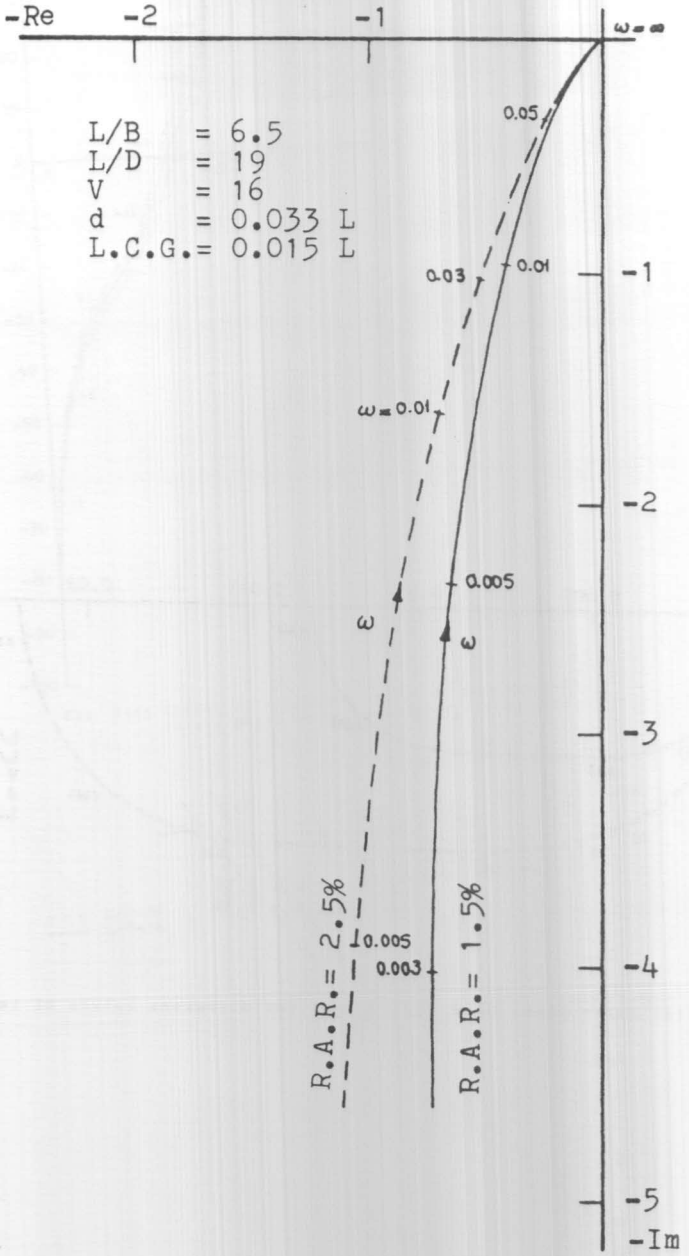

Fig. (15) Polar plots of $\theta_m(jw)/\delta_r(jw)$ for different values of rudder area ratio

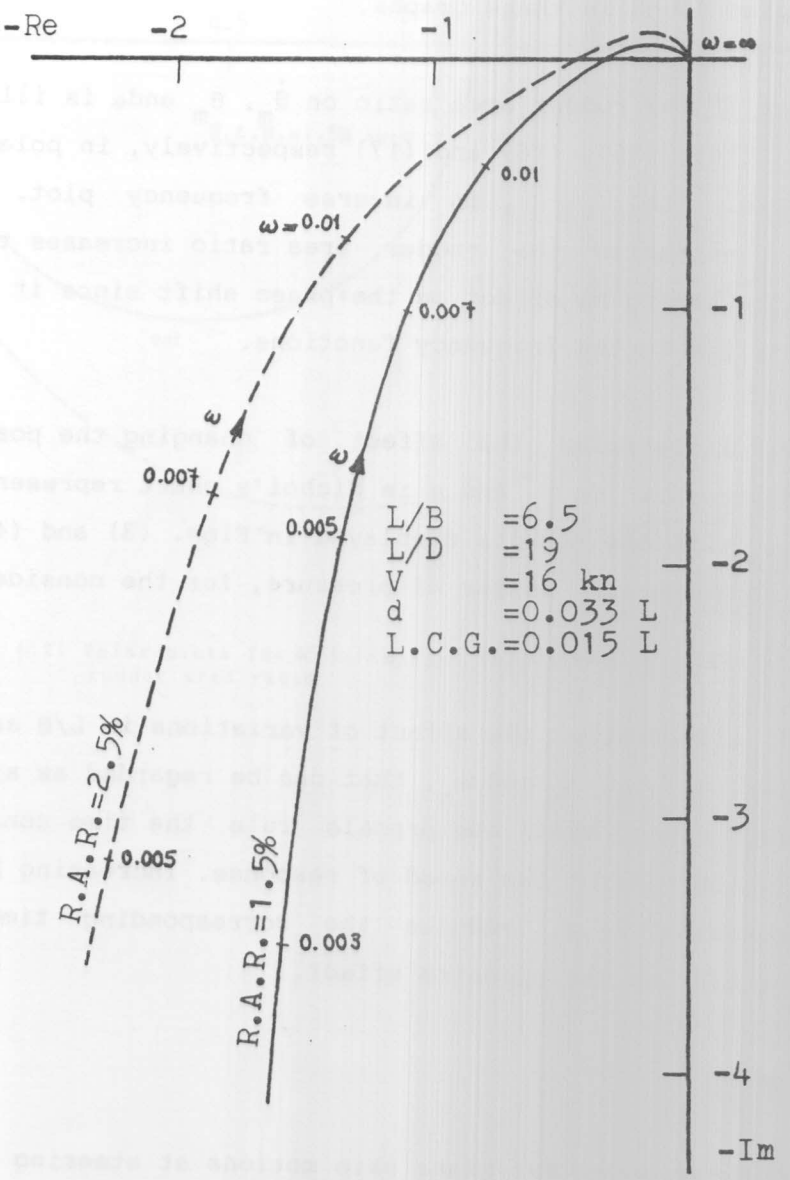

Fig. (16) Polar plotsof $\theta_p(jw)/\delta_r(jw)$ for different values of rudder area ratio

Other frequency response illustrations are shown in Fig. (12) for θ_m in db-magnitude versus phase angle plot, and Fig. (13) for α in inverse frequency plot. The same trend for the effect of L/D on θ_m and α is also found in these graphs.

The effect of the rudder area ratio on $\dot{\theta}_m$, θ_m and α is illustrated in Figs. (14), (15), (16) and (17) respectively, in polar plot form, and in Fig. (18) in inverse frequency plot. From these diagrams, increasing the rudder area ratio increases the magnitude ratio, while having no effect on the phase shift since it represents a real multiplier to the frequency functions.

Fig. (19) illustrates the effect of changing the position of the center of pressure on θ_m and α in Nichol's chart representation. In accordance with the results displayed in Figs. (3) and (4) the effect of the location of center of pressure, for the considered case, is insensible.

Fig. (20) illustrates the effect of variations in L/B and L/D on the frequencies ω_c, ω_d, ω_n and ω_s, that can be regarded as system parameters, since their reciprocals rule the time constants of the system, which control the speed of response. Increasing L/B increases the frequencies, i.e. reduces the corresponding time constants. Increasing L/D has the opposite effect.

5. Conclusion

A mathematical model for plane ship motions at steering is presented. The directional stability was investigated as well as the frequency response of the ship's coupled yaw and sway motions to sinusoidal

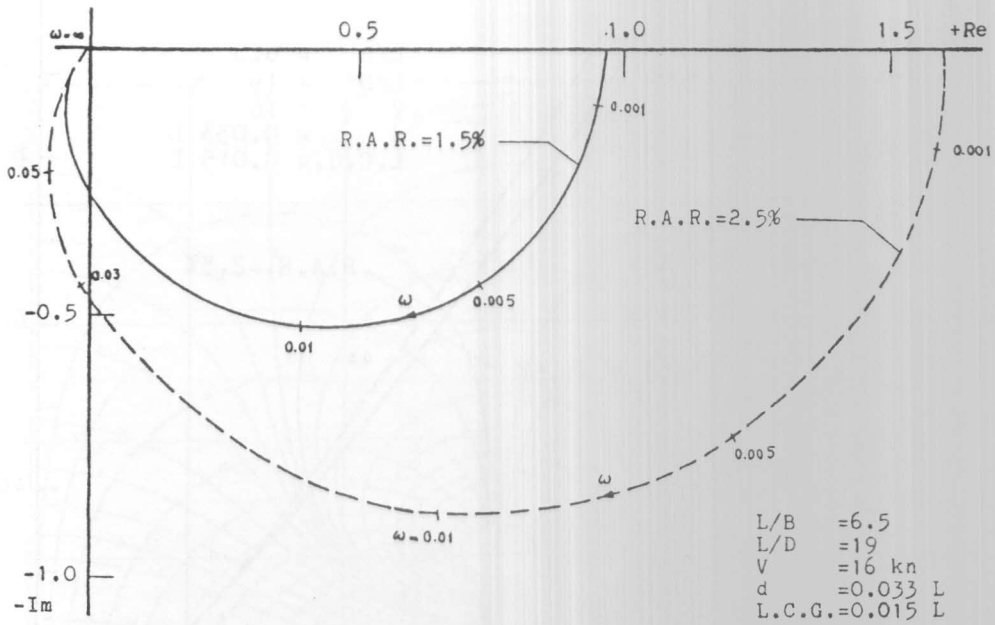

Fig. (17) Polar plots for $\alpha(jw)/\delta_r(jw)$ for different values of rudder area ratio

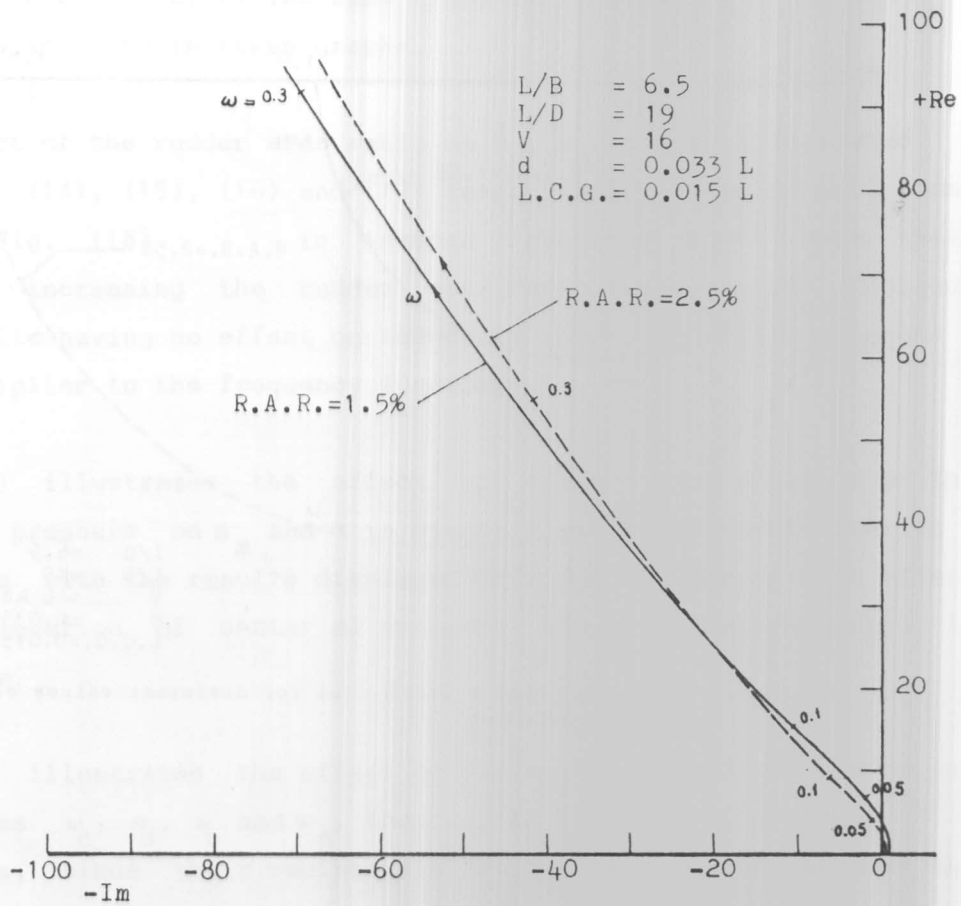

Fig. (18) Effect of variation of rudder area ratio on inverse polar plots of $\alpha(jw)/\delta_r(jw)$

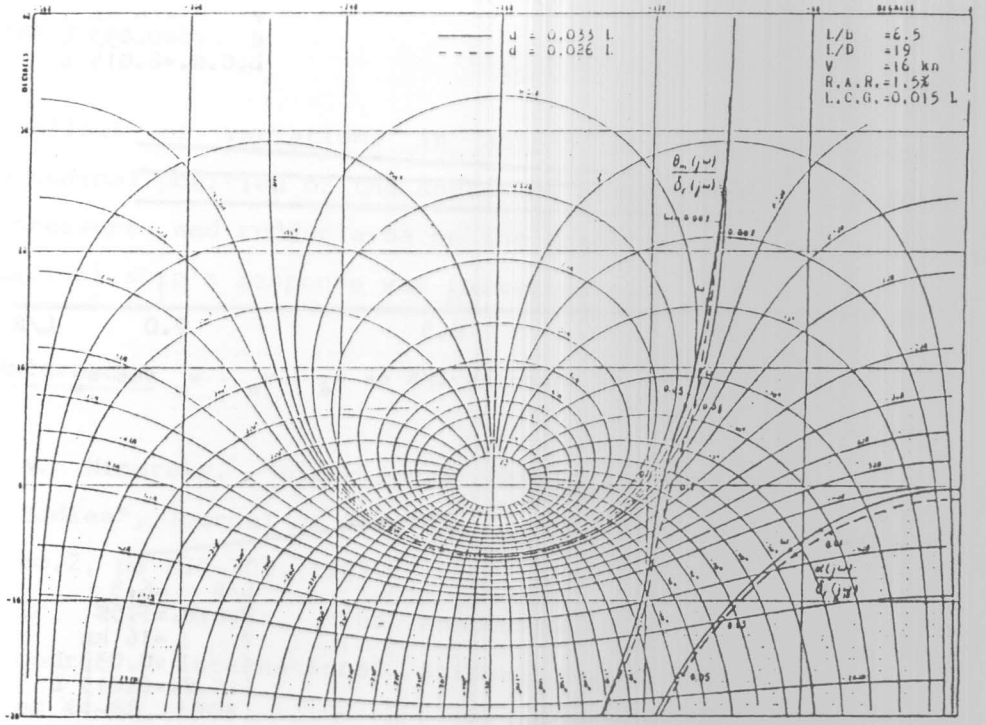

Fig. (19) Effect of variation in the location of the center of pressure on the frequency functions $\theta_m(jw)/\delta_r(jw)$ and $\alpha(jw)/\delta_r(jw)$ on Nichols chart.

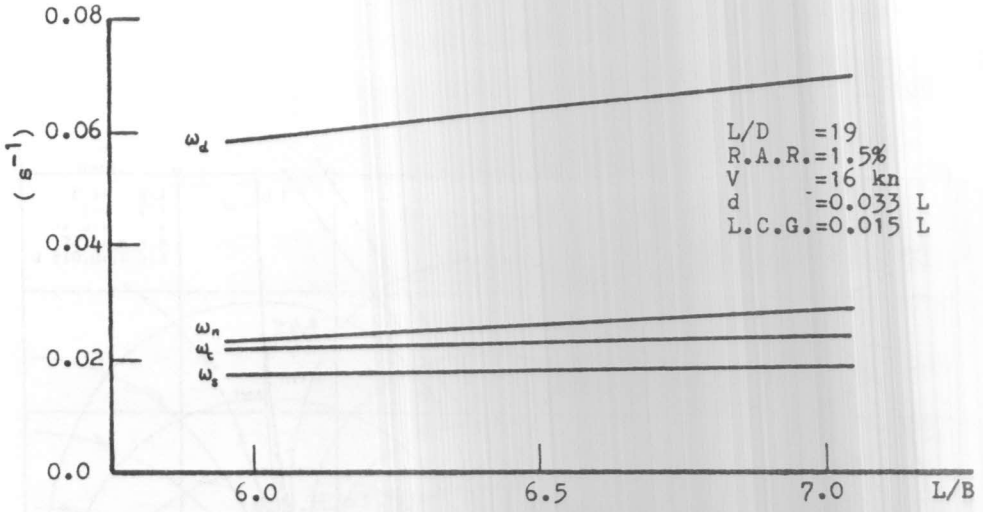

Fig. (20a) Effect of changing L/B on w_d , w_n , w_c and w_s

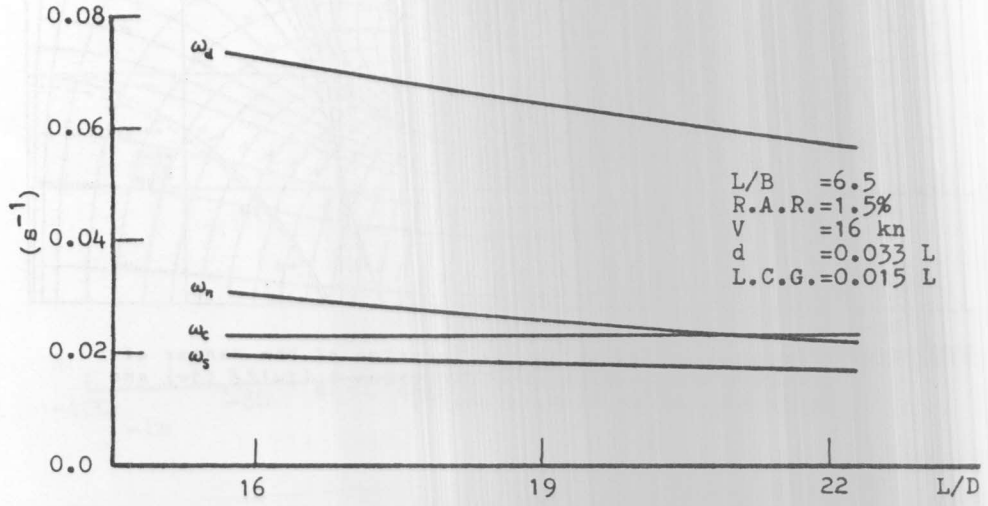

Fig. (20b) Effect of changing L/D on w_d , w_n , w_c and w_s

rudder input at different frequencies. It was shown that the ship's transfer functions behave as a low-pass frequency filter. Both the mathematical model and the interpretation of the results justify the used approximation of the trapezoidal wave by its first harmonic, which, in a Fourier expansion, possesses the maximum amplitude at the lowest frequency.

The effect of variations in ship's principal dimensions' ratios, longitudinal position of the center of gravity, position of the center of pressure and rudder area on the transfer function's poles and the sinusoidal ship's response was investigated.

6. References

[1] N. Minorsky, "Directional Stability of Automatically Steered Bodies", Journal of American Society of Naval Engineers, Vol. 42, no.2, pp 280-309, 1922.

[2] Ir. J.P. Hooft, "The Manoeuvrability of Ships on Straight Course", International Shipbuilding Progress, Vol. 15, no. 162, pp 44-68, 1968.

[3] C.G. Källström and K.J. Åström, "Experiences of System Identification Applied to Ship Steering", Automatica, Vol. 17, no. 1, pp 187-198, 1981.

[4] H. Chestnut and R.W. Mayer, Servomechanisms and Regulating System Design, Vol. I, 2nd Ed., John Wiley & Sons, New York, 1959.

[5] Ir. J. Th. H. Koelink, "Approximate Methods in Z-Steering Test Analysis", International Shipbuilding Progress, vol. 15, no. 162, February 1968.

[6] Doležal and L. Varcop, Process Dynamics, Automatic Control of Steam Generating Plants, Elsevier Pub. Co., Amsterdam, 1970.

[7] W. Oppelt, Ipari Szabályozási Folyamatok Kézikönyve, Műszaki Könyv Kiadó, Budapest, 1969.

[8] H. Chestnut and R.W. Mayer, Servomechanisms and Regulating System Design, vol. II, 2nd Ed., John Wiley & Sons, New York, 1959.

[9] P. Mandel, Ship Manoeuvring and Control, Principles of Naval Architecture, Chapter 8., SNAME, New York, 1967.

[10] W.R. Jacobs, "Estimation of Stability Derivatives and Indices of Various Ship Forms, and Comparison with Experimental Results", Journal of Ship Research, pp 135-163, Sept. 1966.

[11] S. Inoue and others, "Hydrodynamic Derivatives on Ship Manoeuvring," International Shipbuilding Progress, vol. 28, no. 321, 1981.